A Dielectric-Free Superconducting Coaxial Cable

CHRISTOPHER ROSE, MEMBER, IEEE, AND MICHAEL J. GANS

Abstract—We have investigated the theoretical properties of a dielectric-free superconducting coaxial cable with a magnetically levitated inner conductor. We found that at 100 GHz the intrinsic attenuation along such a cable is on the order of a 0.1 dB per kilometer. Furthermore, for a given cable, the loss is proportional to the square of the frequency. Thus, at 10 GHz, one could expect losses on the order of 10^{-3} dB/km. This low loss, coupled with a generous signal to noise ratio ($\approx$ 80 dB at 100 GHz bandwidth), helps provide bit rates of 100 Gbit/s over 600 km. At 10 Gbit/s the distance increases to over 60000 kilometers: about 1.5 times the earth's circumference. Such a high-bandwidth, extremely low loss electronic transmission medium might be of interest for very long distance repeaterless communications. In addition, since efficient means of tapping coaxial media already exist, local area network applications with in excess of 10^4 users could be supported. The two properties of superconductors central to this application are (1) very low intrinsic loss and (2) expulsion of magnetic flux. Low loss allows high-bandwidth dispersionless transmission. Magnetic flux expulsion permits *magnetic support of the inner conductor*, thereby avoiding the large dielectric losses associated with any support material.

I. Introduction

THE CURRENT rage of activity in superconductivity research and the tantalizing hints of room temperature superconductors have sent researchers worldwide scurrying in search of clever uses for superconductive materials. In our own scurrying we investigated the theoretical properties of an ideal superconducting coaxial cable (see Fig. 1) for the transmission of information over large distances (many kilometers). We found that at 100 GHz bandwidth the intrinsic attenuation along such a cable is on the order of 0.1 dB per kilometer. Furthermore, for a given cable, the loss is proportional to the square of the frequency. Thus, at 10 GHz, one could expect losses on the order of 10^{-3} dB/km. This low loss, coupled with a generous signal to noise ratio, provides bit rates of 100 Gbit/s over more than 600 km. At 10 Gbit/s the distance increases to over 60000 kilometers: about 1.5 times the earth's circumference. Such a high-bandwidth, extremely low loss electronic transmission medium might be of interest for very long distance repeaterless communications. In addition, since efficient means of tapping coaxial media already exist, local area network applications with in excess of 10^4 users could be supported in principle.

As a means of realizing such a system, consider an idealized coaxial cable wherein the inner and outer conductors are separated by free space. Such a structure seems implausible since the inner conductor must be mechanically supported. Thus, the more usual structure, in which the space between the inner and outer conductors is filled with some rigid material, was considered. Unfortunately, the insertion of even the best solid dielectrics (i.e., quartz or Teflon) produces losses on the order of 1000 dB/km at 100 GHz. Cleverness such as using only a thin fin of dielectric for support is ineffective in greatly reducing loss. Thus, some other means of mechanical support was sought.

Since superconductors expel all magnetic flux from their interior (Meissner effect) and also offer zero resistance to

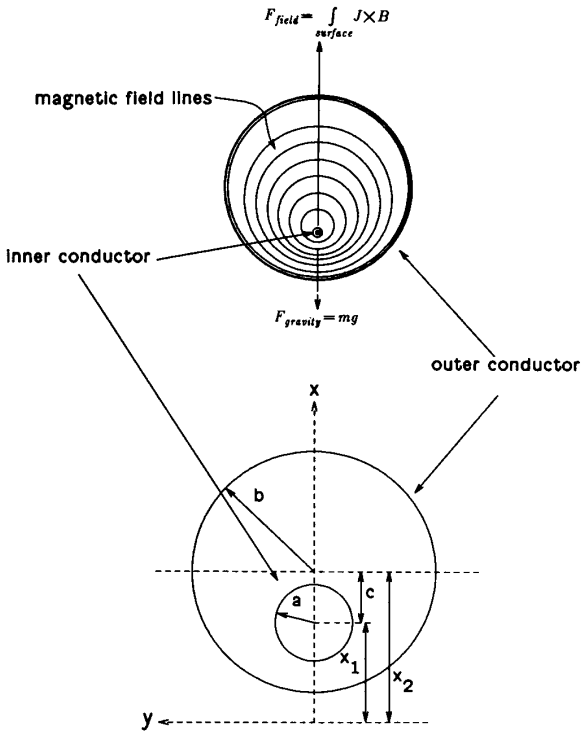

Fig. 1. Schematic representation of idealized coaxial cable. Inner condeuctor (radius a) centered in outer conductor (radius b) and magnetic field between inner and outer conductors produced by current flowing into inner conductor. Lines of magnetic flux are compressed below inner conductor and expanded above. This produces a field gradient over the surface of the inner condeuctor and thereby produces a net force upward.

Manuscript received February 14, 1989; revised August 23, 1989.

The authors are with the Crawford Hill Laboratory, AT&T Bell Laboratories, Holmdel, NJ 07733.

IEEE Log Number 8932000

0018-9480/90/0200-0166$01.00 ©1990 IEEE

dc current flow, we then investigated the possibility of magnetically suspending the inner conductor. We found that the passage of dc current along the inner conductor would be sufficient to stably hold the inner conductor in place with magnetic forces: as if by magic (see Fig. 1). The result is a superconducting coaxial cable with high bandwidth and extremely low loss.

We begin with a brief introduction to the relevant superconductor properties followed by a review of the lumped-element model for coaxial transmission lines. With this background we will calculate the expected losses for ideal and dielectric-filled superconducting coaxial lines. Magnetic levitation of the inner conductor will then be introduced. To help evaluate the efficacy of a superconducting coaxial cable as a communications channel, we will then consider the allowable transmission power from which a signal to noise ratio may be obtained.

II. A Brief Superconductivity Primer

For the new superconductors, any detailed discussion of theoretical properties is partly anecdotal since very little is known about these new materials. In addition, the physics of even the well-known superconductive materials is sufficiently complex that their inclusion here was deemed inappropriate. Thus, we make a number of simplifying assumptions about the new superconductors and the application we propose. The reader desiring more depth is referred to [1]–[5].

For example, we assume that the new superconductor properties are sufficiently similar to those of previously known superconductors, so much of the same theory is applicable. We will also assume that the material is homogeneous (unlike present materials [6], [7]) and that it is never driven into a "mixed" state, wherein nonsuperconducting regions are formed in the material. Consider now a basic macroscopic model of superconducting materials which will allow a quantitative examination of superconductor properties.

A. The London Two-Fluid Model

The basic idea of the London two-fluid model [5] is straightforward. Two types of charge carriers are presumed in superconducting materials: normal electrons, which experience lossy collisions, and superconducting electrons (Cooper pairs), which do not.

The current carried by both types of electrons in a given electric field may be derived from Newton's law $F = ma$. The normal electrons experience an effective viscous drag force of $\nu\bar{v}_n$ opposite to their directions of motion, where $\bar{v}_n$ is the average velocity of the normal electrons and ν is a viscous drag coefficient (N·s/m). All electrons experience a force of $-qE$ when placed in an electric field E ($-q$ being the charge of an electron) so that the total force acting on the normal electrons is

$$F_n = -(\nu\bar{v}_n + qE) = ma_n = m\dot{\bar{v}}_n \tag{1}$$

where m is the electron mass. If we assume that the normal electrons are rapidly accelerated to the point where the viscous drag exactly cancels the force exerted by the electric field, we have

$$\nu\bar{v}_n = -qE. \tag{2}$$

The current density is given by $J_n = -qn_n(T)\bar{v}_n$ where $n_n(T)$ is the normal electron density as a function of temperature, T. Thus,

$$J_n = q^2 n_n(T)E/\nu = \sigma_n(T)E \tag{3}$$

which is the usual Ohm's law.

The corresponding relation for the superconducting electrons is found similarly. Since the electrons experience no viscous drag, we obtain

$$\frac{\partial}{\partial t}(J_{sc}) = \dot{J}_{sc} = n_{sc}(T)q^2E/m = \theta_{sc}(T)E \tag{4}$$

where $n_{sc}(T)$ is the density of superconducting electrons as a function of temperature. Equation (4) may be viewed as Ohm's law for superconductors and resembles the relation between voltage and current through an inductor with $L_{sc} = \theta_{sc}^{-1}(T)$. The temperature dependence of θ_{sc} and σ_n is given by [1], [5]

$$\sigma_n(T) \approx \sigma_{n_0}(T/T_c)^4 \tag{5}$$

$$\theta_{sc}(T) \approx \theta_{sc_0}\left[1-(T/T_c)^4\right]$$

where T_c is the superconducting transition temperature ($T_c \approx 93°\text{K}$ for $YBa_2Cu_3O_{7-x}$ superconductors [8]–[10]). The value of σ_{n_0} has been found to be $\approx 10^5$ mho/m for the YBaCuO superconductors [7], [8], [10].

Armed with (3), (4), and (5), a set of useful relations may be derived from Maxwell's equations. For the sake of brevity, most are simply listed rather than derived. All expressions given can be found in [1].

The propagation constant, k, in a superconducting material is given by,

$$k^2 = \mu\left(\theta_{sc}(T) + j\omega\sigma_n(T) - \omega^2\epsilon\right). \tag{6}$$

The depth to which electromagnetic fields may penetrate (skin depth) is then defined as $\lambda = 1/\text{Re}[k]$.

For normal conductors where $\theta_{sc}(T) = 0$ and $\sigma_n(T)$ isbassumed large, the skin depth is $\sqrt{2/\omega\mu\sigma_n(T)}$. For superconductors θ_{sc} is the dominant term in (6). Thus, using equation (5), we find λ to be

$$\lambda(T) \approx \lambda_0/\sqrt{1-(T/T_c)^4} \tag{7}$$

where $\lambda_0 \approx 10^{-7}$ m [8], [10]. Since $\lambda(T)$ is small and approximately independent of frequency, we see that superconductors exclude virtually all magnetic field from their interior (even at $\omega = 0$). This property, known as the Meissner effect, is one of the tests for true superconductivity [1]–[3], [5].

The intrinsic impedance (surface impedance) of the material, η, may be found by taking the ratio of the electric and magnetic fields perpendicular to the direction of wave propagation [11], [12]. Written in terms of $\lambda(T)$ (for

superconductors) we have

$$\eta = j\omega\mu_0\lambda(T)\sqrt{\frac{1}{1+j\omega\mu\lambda^2(T)(\sigma_n(T)+j\omega\epsilon)}}. \quad (8)$$

Typically, $\mu \approx \mu_0$ for superconductors in the normal state.

B. Superconductor Model Limitations

Of course there are various limitations. One such limitation is on the frequency of field variation, f. The energy, $2\Delta_{gap}$, required to decouple the superconductive paired electrons is on the order of 25 to 30 meV for the YBaCuO superconductors [13]. Thus, photons of frequency $f_{gap} = 2\Delta_{gap}/h$ (where h is Planck's constant) would drive the superconductor completely normal. For frequencies $f > f_{gap}/10$, the superconductive properties begin to degrade so that for the YBaCuO superconductors, the maximum usable frequency is on the order of 1 THz.

Another limitation is on the magnitude of the field to be expelled. Above the critical field, type II superconductors begin to support magnetic flux through their bulk and eventually revert to their nonsuperconducting state [1]–[3]. Present measurements of the critical field, H_{c1}, for the YBaCuO superconductors give $H_{c1} \approx 0.08$ T [8], [10]. The expected theoretical bulk B_{c1} can be calculated using the relation [1]

$$B_{c1} = \frac{\Phi_0}{4\pi\lambda^2(T)}\ln\kappa \quad (9)$$

which is derived from thermodynamic arguments ($\Phi_0 = 2.069\times10^{-15}$ T m^2). The measured value of κ is in the range $40 \le \kappa \le 150$ [8], [10], [14] for the $YBa_2Cu_3O_{7-\delta}$ superconductor. Setting $\lambda(T) = 10^{-7}$ m, we obtain

$$0.06\text{ T} \leqslant B_{c1} \leqslant 0.082\text{ T} \quad (10)$$

which is in agreement with observed behavior.

III. Superconducting Coaxial Cable

A. Lumped Element Model for Coaxial Cable

Consider a coaxial cable with circular cross section. We assume only radial electric fields during transmission (TEM propagation). If the frequency of operation, f, is constrained by

$$f < \frac{2c}{1.873\pi(a+b)} \quad (11)$$

where c is the speed of propagation along the cable and a and b are the inner and outer conductor radii respectively, then only one solution to the field equations (mode) will propagate in the cable [12]. This fundamental mode (TEM mode) mas the property that in the absence of loss, a brief but band-limited voltage pulse will propagate along the cable without distortion. This feature is attractive from the standpoint of information transmission over long distances.

Given that f satisfies (11), a lumped-element transmission line model may be used [11] with C the capacitance per unit length of the cable, G the shunt conductance per unit length through the dielectric, L the inductance per unit length, $V(x)$ the voltage between the conductors, and $I(x)$ the current. Z_{sc} is the intrinsic impedance of the conductor multiplied by a geometric factor.

The values of these parameters in terms of a and b and the material properties are given by

$$C = 2\pi\epsilon/\ln\left(\frac{b}{a}\right) \quad (12)$$

$$G = 2\pi\epsilon\omega\tan\delta/\ln\left(\frac{b}{a}\right) \quad (13)$$

$$L = \frac{\mu_0}{2\pi}\ln\left(\frac{b}{a}\right) \quad (14)$$

$$Z_{sc} = \eta\frac{\left(\frac{1}{a}+\frac{1}{b}\right)}{2\pi}. \quad (15)$$

The values $\tan\delta$, μ_0, and ϵ are defined as the loss tangent of the dielectric, the permeability, and the permittivity, respectively. These values are tabulated for various materials at different frequencies in [15].

If solutions of the form $I(z,t)$, $V(z,t) = Ae^{kz}e^{j\omega t}$ are assumed, then a relation between k and the model parameters can be obtained [11]:

$$k^2 = -\omega^2\mu_0\epsilon(1-j\tan\delta)\left(1+\left(\frac{(1/a+1/b)}{\ln(b/a)}\right)\left(\frac{\eta}{j\omega\mu_0}\right)\right). \quad (16)$$

The real part of k determines the loss of signal energy and the imaginary part of k determines the delay experienced by different frequency components of the signal (delay spread). Both loss and delay spread can induce distortion (i.e., pulse spreading) in a signal traveling along the cable. Such pulse spreading reduces the number of pulses which can be sent during a given time period, which effectively reduces the bandwidth of the cable for a given length.

B. Unsupported Inner Conductor

If the inner conductor of Fig. 1 is assumed to float in free space, then the loss tangent $\tan\delta$ disappears. The propagation constant is then given by

$$k^2 = -\omega^2\mu_0\epsilon_0\left(1+\left(\frac{(1/a+1/b)}{\ln(b/a)}\right)\left(\frac{\eta}{j\omega\mu_0}\right)\right). \quad (17)$$

The expression for η (eq. (8)) may be approximated by noting that $\omega\epsilon \ll 1\sigma_n(T)$ and $\omega\sigma_n(T)\mu\lambda^2(T) \ll 1$. The assumption leads to an expression for the loss factor, $\alpha = \mathrm{Re}[k]$:

$$\alpha \approx \omega^2\sqrt{\mu_0\epsilon_0}\,\mu_0\lambda^3(T)\sigma_n(T)\left(\frac{(1/a+1/b)}{4\ln(b/a)}\right) \quad (18)$$

and phase factor, $\beta \approx \mathrm{Im}[k]$:

$$\beta \approx \omega\sqrt{\mu_0\epsilon_0}\left(1+\lambda(T)\left(\frac{(1/a+1/b)}{2\ln(b/a)}\right)\right). \quad (19)$$

Since β varies linearly with ω to a first approximation, the structure exhibits no delay spread.

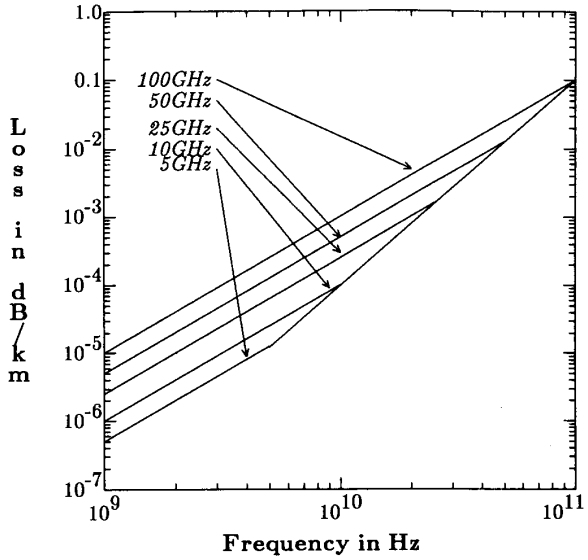

Fig. 2. Loss versus frequency for an ideal superconductive coaxial transmission line. Loss is plotted in dB/km as $20\times10^3\log_{10}e^{\alpha}$, where $\alpha = 0.5372\times\omega^2\omega_{max}\epsilon_0\mu_0^2\lambda_0^3\sigma_{n_0}R(T)$ and $R(T) = (T/T_c)^4(1-(T/T_c)^4)^{-1.5}$. Changes in ω_{max} imply changes in the dimensions of the cable (see eq.(21)). Ratio of outer conductor to inner conductor is assumed fixed at the minimum loss ratio of $b/a = 3.6$, $\epsilon_0 = 8.85\times10^{-12}$F/m, $\mu_0 = 4\pi\times10^{-7}$H/m, $\sigma_{n_0} = 10^5$mho/m, $\lambda_0 = 10^{-7}$m. Plots are made for $T/T_c = 0.5(R(T) = 6.88\times10^{-2})$.

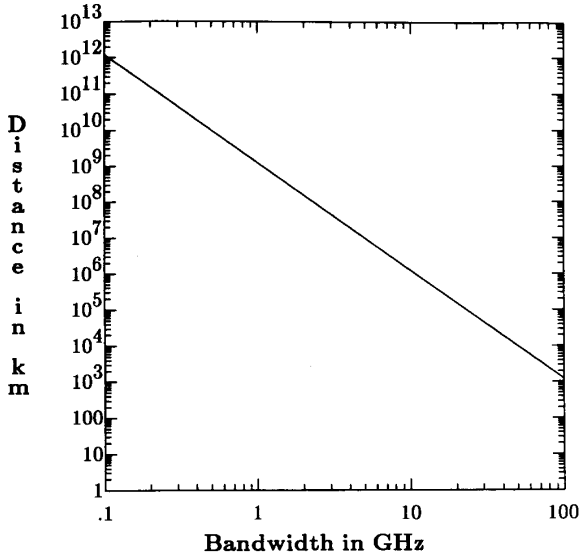

Fig. 3. Distance a Gaussian pulse of bandwidth ω (power in spectrum at ω is down 42.9 dB from its dc level) may travel before doubling in duration. ω_{max} of cable is assumed equal to pulse bandwidth.

To remove the dependence of (18) on physical dimensions a and b, we assume single-mode operation at frequency ω_{max} so that by (11),

$$a + b = 2.1356/\sqrt{\mu_0\epsilon_0}\,\omega_{max}. \tag{20}$$

We then choose $b/a = 3.6$ for minimum loss [12], use (20), and include the temperature dependence given in (5) and (7). Equation (18) then becomes

$$\alpha \approx 0.5372\times\omega^2\omega_{max}\epsilon_0\mu_0^2\lambda_0^3\sigma_{n_0}\left(\frac{T}{T_c}\right)^4\left(1-\left(\frac{T}{T_c}\right)^4\right)^{-3/2} \tag{21}$$

In Fig. 2 we plot the loss, e^{α}, in dB/km versus frequency for various maximum frequencies, ω_{max}. The temperature, T, is assumed to be $T_c/2$ (see caption for further details). For $\omega_{max} = 2\pi\times10^{11}$ rad/s we see that the maximum loss of ≈ 0.1 dB/km occurs at the maximum frequency of 100 GHz. If we assume that a Gaussian pulse propagates along the cable, a related figure of merit is the distance at which the pulse width doubles. For the parameters of Fig. 2, $\omega_{max} = 2\pi\times10^{11}$ and pulse width 10^{-11} s. (100 Gbit/s), the pulse may travel $\approx$1200 km before doubling in width.[1] This maximum useful distance is plotted versus ω_{max} in Fig. 3.

[1]The pulse width is defined to be 2σ, where σ^2 is the variance of the Gaussian pulse. For $\omega\,\max = \pi/\sigma$, the power in the signal at the band edge ($\omega\,\max$) is more than 4 orders of magnitude smaller than the maximum power (at $\omega = 0$). Thus, the signal fits well within the band. A more extensive treatment of Gaussian pulses in dispersive media is provided in Appendix II.

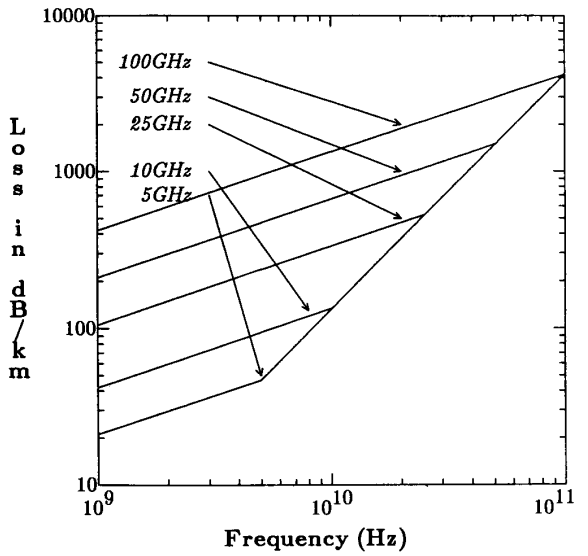

Fig. 4. Loss versus frequency for copper coaxial cable. Loss is plotted in dB/km as $20\times10^3\log_{10}e^{\alpha}$, where $\alpha = 1.074\sqrt{\mu\epsilon\omega_{max}}\,r\omega\epsilon/2\sigma$. $\sigma = 5.96\times10^7$ for copper. Free-space values for ϵ and μ are assumed (see caption to Fig. 2).

For comparison, the much greater loss versus frequency characteristic for copper coaxial cable is provided in Fig. 4.

C. Inner Conductor Supported by Dielectric

In this case the shunt conductance G is nonzero at high frequency. If we assume negligible loss in the conductor we obtain

$$k \approx j\omega\sqrt{\mu_0\epsilon}\left(1-j\frac{\tan\delta}{2}\right). \tag{22}$$

The loss factor due to the dielectric, $\alpha_{\text{dielectric}}$, is then

$$\alpha_{\text{dielectric}} = \omega \frac{\tan\delta}{2} \sqrt{\mu_0 \epsilon} . \tag{23}$$

For a good dielectric such as Teflon with a loss tangent $\approx 6\times10^{-4}$ ($1 \rightarrow 100$ GHz) and a relative dielectric constant of ≈ 2 [15], $\alpha_{\text{dielectric}} = \omega \times 1.41 \times 10^{-12}$. For $\omega_{\max} = 2\pi \times 100$ GHz, $\alpha_{\text{dielectric}}$ is approximately 69000 times greater than the intrinsic loss of the superconducting cable at best. For a 10 GHz cable ($\omega_{\max} = 2\pi \times 10$ GHz), this ratio increases by a factor of 100. It is readily seen that to decrease the dielectric loss by simply using less dielectric would be difficult. For a cable with outer conductor radius 1 mm, reduction of the amount of dielectric by a factor of 69000 results in a supporting dielectric fin 0.023 μm thick. Even if such a thin slice of material could support the inner conductor, other effects, such as the tendency of the wave front propagating down the cable to be directed into the dielectric due to the lower propagation speed in the dielectric, will increase the loss and favor dispersion. Thus, the insertion of any solid dielectric severely degrades the performance of the superconducting cable.[2]

V. Support Without A Dielectric

A. Magnetic Levitation

To avoid the insertion of a lossy dielectric support, we wish to levitate the inner conductor of a coaxial cable in a magnetic field. By passing a dc current through the inner conductor, circular magnetic flux lines between the inner and outer conductors are trapped (Fig. 1). Any movement away from center of the inner conductor will compress flux lines. Since magnetic flux lines resist compression (qualitatively), a restoring force is generated which tends to float the inner conductor. The model of Fig. 1 is treated analytically in Appendix I. However, let us consider a simplified problem from which we can obtain some intuition.

Consider a current line of magnitude I located between (and running parallel to) two superconducting plates separated by $2d$. The superconducting plates will not permit any magnetic flux normal to their surfaces. This boundary condition may be met conceptually using the method of images [1] to place an infinite set of image currents each with magnitude I as shown in Fig. 5. Notice that the direction of the image currents alternate as y increases or decreases. Also notice that current lines traveling in the same direction are separated by $4d$ independent of Δ, the deviation of the original current line from $y = 0$. Thus, we could consider the arrangement of Fig. 5 as two interwoven "combs" of oppositely directed currents.

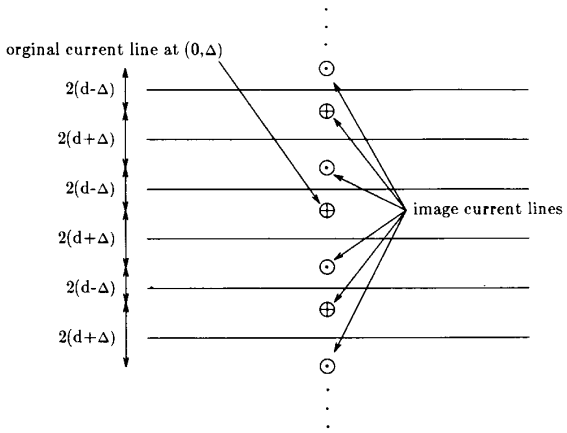

Fig. 5. Image current representation of a current line located between two superconducting plates located at $y = \pm d$. Real current line is located at $y = \Delta$. All other current lines are images.

An intuitive feel for the force exerted on the real current line may be obtained by noting that current lines carrying oppositely directed currents repel whereas current lines carrying current in the same direction attract. These repulsive and attractive forces have a $1/r$ dependence for this axially symmetric geometry. If the tines of the two combs are equidistant then no net force results. If, however, the real current is moved away from $y = 0$, then the mutually repulsive combs are brought closer together and a restoring force is generated. Thus, we might expect that there will be zero force at zero displacement from center and that this force will increase toward ∞ as the current combs grow closer together ($r \rightarrow 0$).

A further observation may be made by considering that superconductors can withstand only limited magnetic field intensities before entering the mixed state or reverting to normal. The field intensity at the surface of the current line is infinite ($r = 0$). Thus, we might expect that if we are to avoid exceeding a given maximum magnetic field ($B_{\max}$) the amount of current passed through the line must be decreased as the line is brought closer to the superconducting plates.

The qualitative effect of this assumption on the force versus displacement curve would be to drive it toward zero rather than ∞ as the line is brought into contact with the superconducting plate. So in total, we should expect an initial increase in restoring force as the line is moved away from center ($\Delta = 0$), peaking at some critical value and then returning to zero as $\Delta \rightarrow d$.

Our qualitative suspicions are verified by calculation of the exact relation between force and displacement for a cylindrical conductor in a cylindrical shell (Appendix I). Plots of the corresponding force versus displacement characteristics for various inner/outer conductor ratios, γ, are shown in Figs. 6 and 7. For a coaxial cable with $b = 0.79$ mm, $a = 0.22$ mm (100 GHz maximum frequency, $\gamma = 1/3.6$), $\Delta = 0.079$ mm, (10 percent displacement from cen-

[2]It should be noted that the properties of a dielectric depend upon temperature as well. Specifically, the loss tangent usually decreases with temperature. For Teflon at 4.2 K the dielectric loss tangent was theoretically approximated as $< 2\times10^{-7}$ [16], a reasonable value for our application. However, dielectric loss is presumed to increase with the square of the temperature so that at liquid nitrogen temperatures (77°) the loss would be $\approx 3.9\times10^{-5}$, which would make the cable at best 4485 times more lossy than the superconducting cable (ω max = 100 GHz): more reasonable than 69,000 but still not acceptable. See [16] for details on the variation of dielectric constant with temperature.

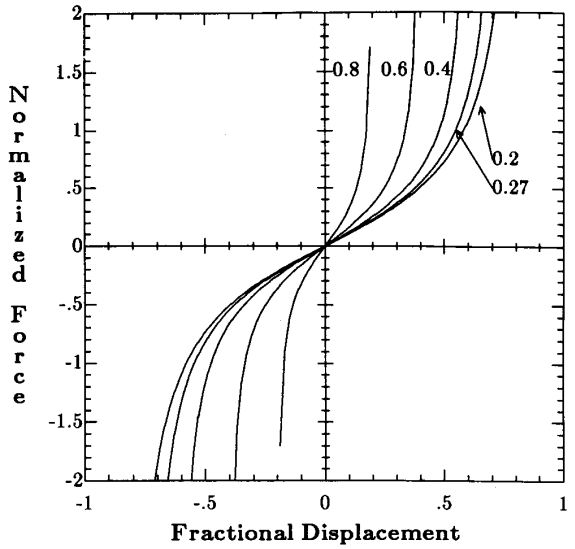

Fig. 6. Exact solution for force on the current-carrying inner conductor of radius a in a cylindrical outer conductor of radius b as a function of displacement, Δ/b. Plots for various inner/outer conductor ratios (γ) are labeled.

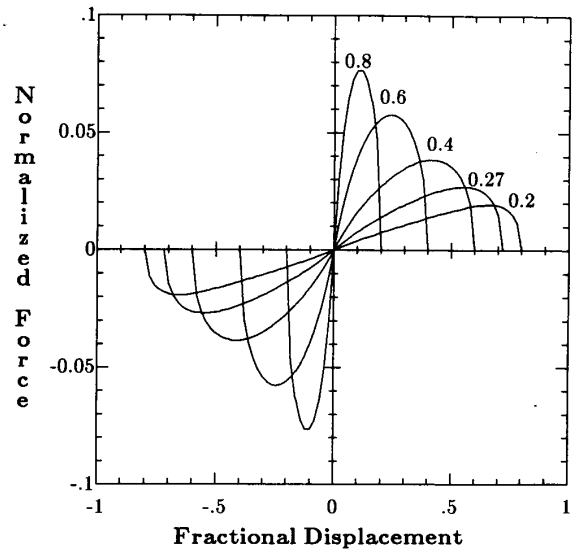

Fig. 7. Exact solution for maximum force on inner conductor as a function of Δ/b.

ter) and an assumed critical field of $B_{max} = 0.06$ T, the maximum restoring force is 0.21 N/m. Thus, with a weight[3] of ≈ 0.01 N/m the inner conductor can be kept well within a 10 percent displacement from center and requires 0.013 T to be kept at exactly 10 percent.

[3]The new superconductors are approximately 6.5 times as dense as water assuming a $3.821 \times 3.900 \times 11.68$ Å orthorhombic crystal structure and the chemical formula $YBa_2Cu_3O_7$ [8]. Thus, a YBaCuO rod of radius 0.22 mm would weigh 9.8×10^{-4} kg/m and generate a force on earth of about 0.01 N/m. For comparison, silver is 10.5 times as dense as water, lead 11.35 times [19].

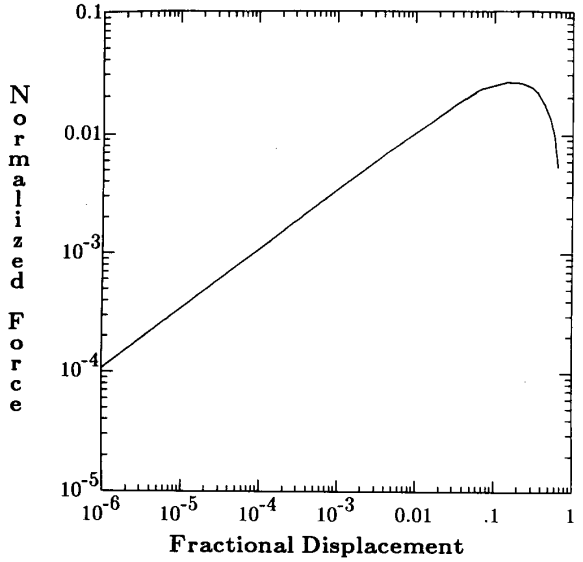

Fig. 8. Maximum force on inner conductor (data of Fig. 7 with $\gamma = 1/3.6$) plotted versus inner conductor displacement from outer conductor (inner conductor is resting against outer conductor for abscissa = 0). Displacement is normalized by outer conductor radius b.

B. Levitation from Initial Rest

With no dc current flowing, most of the inner conductor of the cable will rest against the outer conductor. This raises the question of how the inner conductor can be levitated into place from initial rest. The magnetic field imposed upon the inner conductor when current is applied varies from infinity at the first point of contact between the inner and outer conductors to under B_{cl} on the opposite side of the inner conductor. As a worst case we may assume that when B_{cl} is exceeded, the material reverts to its normal state and effectively ceases to conduct. We then ask, how much of the inner conductor is rendered normal by the intense magnetic field? Or, equivalently, we may ask at what point in the inner conductor does the field strength drop below B_{cl}? If this distance is small relative to the diameter of the inner conductor, then we can argue that the nonconducting region may be ignored (assumed absent or ablated) with little total effect on the field. For analytical purposes, this scenario corresponds to levitating the inner conductor, assuming some initial displacement (and thus noninfinite field strengths). We now determine the separation at which enough force exists for levitation while the peak magnetic field is maintained below B_{cl}.

Consider Fig. 8, which is a logarithmic plot of the maximum force versus displacement for a coaxial cable with outer conductor radius 3.6 times that of the inner conductor. The abscissa differs slightly from that of Fig. 7 in that zero displacement corresponds to the inner conductor in contact with the outer conductor and a displacement of 1 implies that the inner conductor is centered. Again assuming that $a = 0.22$ mm and $b = 0.79$ mm, the inner conductor weighs approximately 0.01 N/m. If we assume a critical field of $B_{max} = 0.06$ T, then the corresponding

normalized forces in Fig. 8 is $\approx 3.5\times10^{-4}$. We thus find the initial displacements above $\approx 10^{-5}b$ will allow the inner conductor to be lifted toward center. A displacement of $10^{-5}b$ corresponds in this case to an initial offset of only 79 Å. Thus, using the argument of the preceding paragraph, levitating the inner conductor into place from initial rest should not prove to be a problem.

V. Signal/Noise and Maximum Repeaterless Distance

An important figure of merit for any transmission medium is the distance a signal may travel and still be correctly detected at the receiver. Aside from pulse spreading, the relevant factors are

1) acceptable error rate: ϵ,
2) receiver noise: n_R,
3) intrinsic transmission medium noise: n_m,
4) signal power at receiver: P_s,
5) signal attenuation with distance: α.

A. Error Rate and Noise Sources

Let us assume that all noise processes are white and Gaussian over the frequency band of interest. Furthermore, set the acceptable bit error rate (BER) to 10^{-9}. The signal power to noise power ratio (SNR) necessary to achieve this BER is approximately 36 (on/off keying) [20]. If we assume a receiver whose impedance is matched to the impedance of the cable, we obtain a receiver noise power of

$$n_R = kT\Delta f \tag{24}$$

where k is the Boltzman constant (1.38×10^{-23} J/K), T is the temperature, and Δf is the signal bandwidth [21].

Since large dc currents are necessary to magnetically support the inner conductor of the coaxial cable, we may expect in the worst case a noise contribution from statistical variation in the dc current, I_{dc} (shot noise). This noise will manifest itself to the receiver by its accompanying electric field (voltage) of magnitude $V = I_{noise}Z_{cable}$ where

$$Z_{cable} = \sqrt{L/C} = \frac{\ln(b/a)}{2\pi}\sqrt{\mu/\epsilon}. \tag{25}$$

The rms value of I_{noise} is $\sqrt{2qI_{dc}\Delta f}$, where $q = 1.602\times10^{-19}$C is the electronic charge. Thus,

$$n_I = (qI_{dc}\Delta f)\frac{\ln(b/a)}{\pi}\sqrt{\mu/\epsilon}. \tag{26}$$

B. Power Capacity of Cable

Electrical arcing and critical field, B_{c1}, limit the power which may be carried by the cable. From subsection IV-A we see that a field of 0.013 T will hold the inner conductor ($b = 0.79$ mm, $a = 0.22$ mm) to within 10 percent of center. This dc field of 0.013 T corresponds to a dc current of 13.5 A (Appendix I).

The E field should not exceed the breakdown field of air (3.0×10^6 V/m [11]), which, if we allow a factor of 2 margin, suggests $E_{sig} \leqslant 1.5\times10^6$ V/m. Likewise, let the critical field, B_{c1}, have a theoretical value of 0.06 T. With 0.013 T used to support the inner conductor and again assuming a safety factor of 2, we obtain $B_{sig} \leqslant 0.024$ T.

Since,

$$E = H\sqrt{\frac{\mu_0}{\epsilon}} = \frac{B}{\sqrt{\mu_0\epsilon}} \tag{27}$$

we have

$$\left(E_{sig} < 1.5\times10^6 \text{ V/m}\right) \rightarrow \left(B < 0.005 \text{ T}\right) \tag{28}$$

$$\left(B_{sig} < 0.024 \text{ T}\right) \rightarrow \left(E < 7.18\times10^6 \text{ V/m}\right).$$

Thus, the power is electric field limited.

The total signal power carried by the coaxial cable with peak field $E_{sig} = 1.5\times10^6$ V/m is then [12]

$$P_{sig} = \frac{1}{2}(E_{sig}a)^2 2\pi \ln\frac{b}{a}\sqrt{\epsilon/\mu_0} = 1.16 \text{ kW}. \tag{29}$$

C. Maximum Repeaterless Distance

The total signal to noise ratio is

$$\text{SNR} = \frac{P_s}{n_R + n_I}. \tag{30}$$

Assuming a temperature of $T = 300$ K and a signal bandwidth of $\Delta f = 10^{11}$ Hz, (24) gives $n_R = 4.14\times10^{-10}$ W. If $I_{dc} = 13.5$ A and $b/a = 3.6$, then $n_I = 3.32\times10^{-5}$ W. Therefore, the available signal to noise ratio is limited by the dc current shot noise. Evaluation of (30) yields

$$\text{SNR}_{max} = 5\times10^7 \approx 77 \text{ dB}. \tag{31}$$

Thus, for a BER of 10^{-9} a link margin of $1.39\times10^6 = 61.4$ dB is obtained. This implies that a 100 GHz signal (which by Fig. 6 has 0.1 dB/km attenuation) may travel ≈ 614 km without amplification or that the cable may be tapped 10^6 times in principle.

TABLE I
Comparison of Superconductor Properties

-	$YBa_2Cu_3O_{7-x}$	Niobium(Nb)	Lead(Pb)
T_c(°K)	93	9.25	7.2
σ_{n_0}(mho/m)	10^5	8×10^6	5×10^6
H_c, H_{c1}(Tesla)	0.08	0.2	0.08
λ_0(meters)	10^{-7}	0.39×10^{-7}	0.37×10^{-7}
relative loss	1	4.7	2.5

VI. Discussion

A. Comparison to Normal Superconductors

It is worthwhile to note some of the differences between the new superconductors and the old (aside from transition temperature). For example, consider the values given for niobium (Nb), and lead (Pb) [1] in Table I. Of particular importance are the differences in skin depth, λ_0, and resistivity, σ_{n_0}, since they affect the loss, α, as given by

(18). For a given coaxial structure operating at a given frequency and temperature (normalized to T_c), the relative loss is given on the last line of the table. We see that the older superconductors with their more shallow skin depths and higher normal conductivities would have about the same loss as the newer high-temperature superconductors although the mechanism by which the low loss is achieved is different for the lower temperature superconductors. Specifically, their shallow penetration depths offset their high conductances, whereas for the high-T_c material, its markedly lower conductance offsets its larger penetration depth. Also note that a superconductor such as niobium is more suited to the levitation process since its critical field is substantially larger.

B. Mechanoelectric Considerations

The interactive effects of mechanical vibration and electrical signal variation (i.e., temporal signal variation) may cause instabilities in the mechanical support. Vibration will certainly cause spurious electrical signal propagation as well as possible mechanical instability.

The issue of mechanoelectric coupling is probably not troublesome, however. By examining Fig. 7 we see that the restoring force acting on the mass of the inner conductor may be modeled by a Hookean spring attached to a mass. For $b = 0.79$ mm, $a = 0.22$ mm, and 10 percent displacement, we find the necessary current to be 13.5 A. The spring constant value[4] is then $k = 126.6$ (N/m)/m. The mass of the inner conductor is $m = 9.88 \times 10^{-4}$ kg/m. Therefore, the mechanical resonant frequency of the system is $f_{res} = \sqrt{k/m}/2\pi \approx 60$ Hz. Thus, if signal components below, say, 100 Hz are prohibited (filtered), then the problem of introducing instability into the mechanical support by electrical signal variation should be eliminated and likewise any spurious signal due to mechanical resonances near 60 Hz would be ignored.

However, environmental vibrations near the resonant frequency could prove troublesome since they might introduce mechanical instability or possibly impedance variations along the cable, which could foster dispersion. Since environmental vibrations in the tens of Hz range are likely, some means of either isolating the cable and/or damping the resonant response may be necessary.

A strictly mechanical consideration is the stiffness of the inner conductor. If the inner conductor is stiff, then any bending of the cable will force the inner conductor against the sheath wall at some point farther along the cable (since the magnetic levitation force would be unable to overcome the inner conductor stiffness). Thus, the inner conductor should be flexible.

C. A Brief Comparison to Optical Fiber Communication

The results of our analysis beg a comparison to lightwave communications. Thus, Fig. 9 shows plots of theoretical bit rate versus distance for an optical fiber and the superconducting coaxial cable. Theoretically, superconducting coaxial cable compares favorably with *currently available* optical fiber [22] for point-to-point transmission at 100 GHz. At 10 GHz, however, where optical fiber is loss limited, coaxial cable loss is still proportional to f^2. Thus, superconducting coaxial cable has the potential to carry multi-GHz bandwidths over tens of thousands of kilometers. Coaxial cable also has the advantage of being able to support a large number of taps (10^6) owing to its large signal to noise ratio.[5] Currently, the number of taps in a fiber optical system is limited to hundreds [23], [24]. This feature might be useful for distribution in a local area network. In addition, rapidly tunable (frequency agile) receivers and transmitters are currently available in the 100 GHz frequency range for electronics whereas no such devices yet exist for optical communications. Nonetheless, whether these seeming advantages can simplify the design of certain types of communication systems is not presently known.

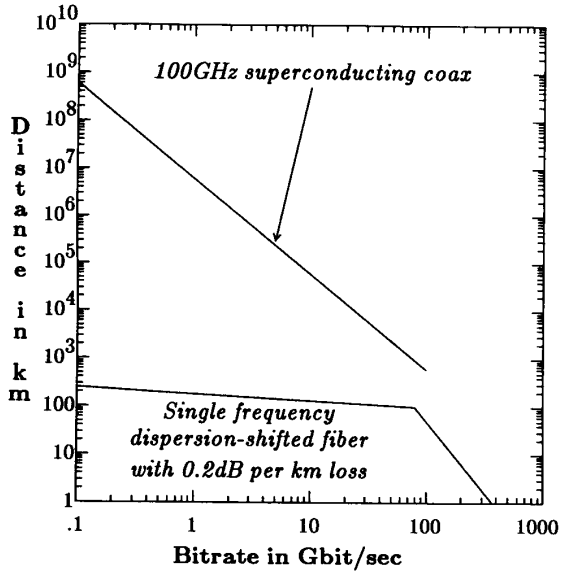

Fig. 9. Bit rate versus distance for various optical fibers and superconducting coaxial cable with bandwidth $\omega_{max} = 2\pi \times 10^{11}$ (100 GHz).

Furthermore, consider that any communications application such as a local area network would probably require room-temperature (or higher) superconductors and, in addition, that a host of other difficult material processing problems be solved. Nonetheless, it is interesting to consider the possibilities, especially in the light of the intense superconducting materials research effort.

VII. Conclusions

We have shown that a coaxial cable constructed from the new high-T_c superconductors could in principle carry high information rates over large distances (100 Gbit/s over 600 km, 10 Gbit/s over 60,000 km). A generous link

[4] k is taken from the slope of the force versus displacement curve at zero displacement.

[5] ≈ 60 dB margin at 100 GHz bandwidth assuming a 10^{-9} bit error rate.

margin of 60 dB (100 GHz at 10^{-9} bit error rate) would allow up to 10^6 taps in principle. The primary feature of the cable design is the support of the inner conductor by magnetic forces. This inovation allows the exclusion of dielectric material for the mechanical support and thereby greatly reduces loss. Such a cable might find utility in long-distance repeaterless communications or in a distributed local area network where low loss, high bandwidth, and the ability to provide a large number of taps are important.

Appendix I
A Cylindrical Conductor Supported in a Cylindrical Shell (Properties of Asymmetric Biaxial Lines)

In this appendix we compute the forces on the center conductor of coaxial lines with a displaced center conductor (biaxial lines). In addition we also determine expressions for the propagation characteristics of such a line. Fig. 1 shows the cross section of an asymmetrical coaxial line. The outside diameter of the center conductor is $2a$ and the inside diameter of the outer conductor is $2b$. The axis of the center conductor is displaced a distance c from the axis of the outer conductor.

We assume perfect conductors with a transverse electromagnetic wave (TEM) of radian frequency ω (which may be zero, dc) propagating down the line. Then, from [25], the electric and magnetic fields are given by

$$\vec{E} = \frac{\eta IA}{\pi} \frac{\left[\hat{x}\left(x^2 - A^2 - y^2\right) + \hat{y}2xy\right]}{\left[(x-A)^2 + y^2\right]\left[(x+A)^2 + y^2\right]} \cdot e^{j(\omega t - kz)} \text{ V/m} \quad \text{(A1)}$$

and

$$\vec{H} = \frac{-IA}{\pi} \frac{\left[\hat{x}2xy - \hat{y}\left(x^2 - A^2 - y^2\right)\right] e^{j(\omega t - kz)}}{\left[(x-A)^2 + y^2\right]\left[(x+A)^2 + y^2\right]} \text{ A/m.} \quad \text{(A2)}$$

The total current in the center conductor is IA; $\eta = \sqrt{\mu_0/\epsilon_0}$ Ω is the free-space impedance; and $k = \omega\sqrt{\mu_0\epsilon_0}$ rad/m is the free-space propagation constant. The constant, A, is defined by

$$A = \sqrt{x_1^2 - a^2}, \qquad x_1 = \frac{b^2 - c^2 - a^2}{2c}. \quad \text{(A3)}$$

The origin of the coordinate system $\{x, y\}$ is displaced a distance x_1 from the axis of the center conductor. When the center conductor is a superconductor, it will require the magnetic flux at its surface to be maintained at less than a critical amount. The maximum magnetic flux occurs at the center conductor where it is closest to the outer conductor and is given by

$$B_{\max} = \mu_0 H_{\max} = \frac{\mu_0 I}{2\pi a}\sqrt{\frac{x_1 + a}{x_1 - a}} \text{ T} \quad \text{(A4)}$$

where μ_0 is the free-space permeability, $4\pi \times 10^{-7}$ H/m. Equation (A4) can then be used to determine the maximum allowable total current, I.

Due to the asymmetry, the current in the center conductor in combination with the magnetic field will experience a net force in the x direction, attempting to move the center conductor back to the center of the outer cylinder. This force can be computed by integrating $\vec{J}_1 \times \vec{B}_1$ around the center conductor, where we introduce the dimensionless variables

$$\gamma \equiv \frac{a}{b}: \text{ ratio of inner conductor radius to outer conductor radius} \quad \text{(A5a)}$$

$$\Delta \equiv \frac{c}{b}: \text{ relative displacement of inner conductor from center of outer conductor} \quad \text{(A5b)}$$

so that

$$\vec{F} = \hat{x}\frac{B_{\max}^2 4\pi b \Delta \gamma^2}{\mu_0} \frac{\sqrt{1-(\Delta+\gamma)^2}}{\left[1-(\gamma-\Delta)^2\right]^{3/2}}. \quad \text{(A6)}$$

The characteristic impedance of the transmission line is the ratio of total voltage, V, to total current, I. The voltage is the line integral of the electric field from inner to outer conductor (since $\nabla \times \vec{E})_z = 0$ the integral is independent of the path in the transverse plane). The resulting characteristic impendance is

$$Z_c = \frac{\eta}{2\pi} \ln\left\{ \frac{\left[\sqrt{(1-\Delta)^2 - \gamma^2} - \sqrt{(1+\Delta)^2 - \gamma^2}\right] \cdot \left[\sqrt{1-(\Delta+\gamma)^2} + \sqrt{1-(\gamma-\Delta)^2}\right]}{\left[\sqrt{(1-\Delta)^2 - \gamma^2} + \sqrt{(1+\Delta)^2 - \gamma^2}\right] \cdot \left[\sqrt{1-(\Delta+\gamma)^2} - \sqrt{1-(\gamma-\Delta)^2}\right]} \right\}. \quad \text{(A7)}$$

To compute the attenuation due to imperfectly conducting walls with a surface resistivity, R_s, we integrate the conductor losses over the conductor perimeters, assuming the current densities associated with a lossless coaxial line [25]. The attenuation coefficient is the ratio of these conductor losses, W_L, to twice the transmitted power, W_T:

$$\alpha = \frac{W_L}{2W_T} = W_L = \frac{R_s I^2}{4\pi b} \frac{(1-\gamma)\left[(1+\gamma)^2 - \Delta^2\right]}{\gamma\sqrt{\left[1-(\Delta+\gamma)^2\right]\left[1-(\gamma-\Delta)^2\right]}} \text{ Np/m.} \quad \text{(A8)}$$

Appendix II
Dispersion Properties of Transmission Lines

In order to compare the bandwidth capacity of various transmission lines it is useful to compute the length of line that will spread a Gaussian pulse of a given duration to double its width. We assume a band-pass Gaussian input pulse

$$f(t) = (\cos\omega_0 t)\exp\left(-t^2/2\tau^2\right). \quad \text{(A9)}$$

The full -4.34 dB ($=1/e$) width of pulse power envelope, $\exp(-t^2/\tau^2)$, is 2τ s. The RMS duration [27] of the pulse power, $f^2(t)$, is

$$t_r = 2\sqrt{\left(\frac{m_{2_f}}{m_{0_f}} \frac{m_{1_f}}{m_{0_f}}\right)^2} = \tau\sqrt{2 - \frac{4\omega_0^2\tau^2\exp(-\omega_0^2\tau^2)}{1+\exp(-\omega_0^2\tau^2)}} \quad \text{(A10)}$$

where moments of $f^2(t)$ are

$$m_{0_f} \equiv \int_{-\infty}^{\infty} f^2(t)\,dt = \frac{\sqrt{\pi}}{2}\tau\left[1+\exp(-\omega_0^2\tau^2)\right]$$

$$m_{1_f} = \int_{-\infty}^{\infty} t f^2(t)\,dt = 0$$

$$m_{2_f} \equiv \int_{-\infty}^{\infty} t^2 f^2(t)\,dt = \frac{\sqrt{\pi}}{4}\tau^3\left[1+(1-2\omega_0^2\tau^2)\exp(-\omega_0\tau^2)\right]$$

For narrow-band signals $\omega_0\tau \gg 1$, $t_r \approx \sqrt{2}\,\tau$, which is the RMS duration of the pulse power envelope. The spectrum of the input pulse is give by its Fourier transform:

$$F(\omega) = \int_{-\infty}^{\infty} f(t)e^{-j\omega t}\,dt$$

$$= \sqrt{\frac{\pi}{2}}\,\tau\left\{\exp\left[-(\omega-\omega_0)^2\frac{\tau^2}{2}\right] + \exp\left[-(\omega+\omega_0)^2\frac{\tau^2}{2}\right]\right\} \quad \text{(A11)}$$

with its inverse

$$f(t) = \frac{1}{2\pi}\int_{-\infty}^{\infty} F(\omega)e^{j\omega t}\,dt. \quad \text{(A12)}$$

We divide $F(\omega)$ into its positive and negative frequency parts, $F_1(\omega)$ and $F_2(\omega)$, respectively:

$$F(\omega) = F_1(\omega) + F_2(\omega)$$

$$F_{1,2}(\omega) \equiv \sqrt{\frac{\pi}{2}}\,\tau\exp\left[-(\omega+\omega_0)^2\frac{\tau^2}{2}\right]. \quad \text{(A13)}$$

The bandwidth of power spectrum around ω_0 where the power, $[F_1(\omega)]^2$, is greater than its peak value divided by e is, using (A10),

$$\text{BW}_{1/e} = \frac{1}{\pi\tau} \approx \frac{\sqrt{2}}{\pi t_r}\text{Hz}. \quad \text{(A14)}$$

When the signal is passed through a transmission line with transmission coefficient $H(\omega)$, the Fourier transform, $G(\omega)$, of the output pulse is the product, $F(\omega)H(\omega)$. For narrow bandwidth, $\omega_0\tau \gg 1$, we can divide the product into positive and negative frequency parts:

$$G(\omega) = G_1(\omega) + G_2(\omega) \qquad G_1(\omega) \approx H_1(\omega)F_1(\omega)$$
$$G_2(\omega) \approx H_2(\omega)F_2(\omega) \quad \text{(A15)}$$

where $H_1(\omega)$ represents the transmission coefficient near $\omega = \omega_0$, and $H_2(\omega)$ that near $\omega = -\omega_0$. Since we are considering real signals,

$$G(-\omega) = G^*(\omega) \quad \text{or} \quad G_2(-\omega) = G_1^*(\omega). \quad \text{(A16)}$$

The Fourier transform of the output pulse power, $g^2(t)$, is [27, p. 27]

$$G_s(\omega) = \frac{1}{2\pi}\int_{-\infty}^{\infty} G\left(y+\frac{\omega}{2}\right)G^*\left(y-\frac{\omega}{2}\right)dy. \quad \text{(A17)}$$

The moments of the output pulse power can be found from the behavior of $G_s(\omega)$ near $\omega = 0$ [27, p. 16]:

$$m_0 = G_s(0) \qquad m_1 = j\frac{dG_s(0)}{d\omega} \qquad m_2 = -\frac{d^2G_s(0)}{d\omega^2}. \quad \text{(A18)}$$

Since we only require $G_s(\omega)$ near $\omega = 0$, for a narrow-band pulse, using (A16),

$$G_s(\omega) \approx \frac{1}{2\pi}\left\{\int_{-\infty}^{\infty} G_1\left(y+\frac{\omega}{2}\right)G_1^*\left(y-\frac{\omega}{2}\right)d\omega + \int_{-\infty}^{\infty} G_2\left(y+\frac{\omega}{2}\right)G_2^*\left(y-\frac{\omega}{2}\right)d\omega\right\}$$

or

$$G_s(\omega) \approx \frac{1}{\pi}\left\{\int_{-\infty}^{\infty} G_1\left[y+\frac{\omega}{2}\right]G_1^*\left[y-\frac{\omega}{2}\right]d\omega\right\}. \quad \text{(A19)}$$

Let us define the transmission line transfer coefficient $H_1(\omega)$ near ω_0 as a third-order expansion of its exponent:

$$H_1(\omega) = \exp\left[\alpha_0 + j\theta_0 + (\alpha_1 + j\theta_1)(\omega-\omega_0) + (\alpha_2 + j\theta_2)(\omega-\omega_0)^2 + j\theta_3(\omega-\omega_0)^3\right]. \quad \text{(A20)}$$

Note that α_3 is set equal to zero to avoid exponential gain for either $\omega \gg \omega_0$ or $\omega \ll \omega_0$. Then we have

$$G_1\left(y+\frac{\omega}{2}\right) = \sqrt{\frac{\pi}{2}}\,\tau\exp\left[\alpha_0 + j\theta_0 + (\alpha_1 + j\theta_1)\left(y-\omega_0+\frac{\omega}{2}\right) + \left(\alpha_2 + j\theta_2 - \frac{\tau^2}{2}\right)\left(y-\omega_0+\frac{\omega}{2}\right)^2 + j\theta_3\left(y-\omega_0+\frac{\omega}{2}\right)^3\right] \quad \text{(A21)}$$

and with $x \equiv y - \omega_0$,

$$G_1\left(y+\frac{\omega}{2}\right)G_1^*(y-\omega/2) = \frac{\pi}{2}\tau^2\exp\left[2\alpha_0 + 2\alpha_1 x + j\theta_1\omega + 2\left(\alpha_2 - \frac{\tau^2}{2}\right)\left(x^2 + \frac{\omega^2}{4}\right) + 2j\theta_2 x\omega + j\theta_3\left(3x^2\omega + \frac{\omega^3}{4}\right)\right]. \quad \text{(A22)}$$

Substituting (A22) into (A19) and integrating [26],

$$G_s(\omega) = \frac{\sqrt{\pi}\tau^2}{2\sqrt{\tau^2 - 2\alpha_2 - 3j\tau_3\omega}} \cdot \exp\left[2\alpha_0 + j\theta_1\omega + \left(\frac{\alpha_2}{2} - \frac{\tau^2}{4}\right)\omega^2 + j\theta_3\frac{\omega^3}{4} + \frac{(\alpha_1 + j\theta_2\omega)^2}{\tau^2 - 2\alpha_2 - 3j\theta_3\omega}\right]. \quad \text{(A23)}$$

Using (A18) we obtain the moments and the RMS duration of $g^2(t)$:

$$t_{rg} = 2\left\{\frac{\tau^2}{2} - \alpha_2 + \frac{2\theta_2^2}{\tau^2 - 2\alpha_2} + \frac{24\alpha_1\theta_2\theta_3 + 9\theta_3^2}{2(\tau^2 - 2\alpha_2)^2} + \frac{18\alpha_1^2\theta_3^2}{(\tau^2 - 2\alpha_2)^2}\right\}^{1/2} \quad \text{(band pass)}. \quad \text{(A24)}$$

This formula is of interest because it shows the combined effect of attenuation and phase coefficients on pulse broadening. Thus, if the transmission line causes $t_{rg} = 2\sqrt{2}\,\tau$, it has doubled the width of the input pulse. The derivation of the above results for a baseband pulse, $\exp(-t^2/2\tau^2)$, gives the same results except a transmission line has a real bandband impulse response, whence $\theta_0 = \alpha_1 = \theta_2 = 0$, and

$$t_{rg} = 2\left\{\frac{\tau^2}{2} - \alpha_2 + \frac{9\theta_3^2}{2(\tau^2 - 2\alpha_2)^2}\right\}^{1/2} \quad \text{(baseband)}. \quad \text{(A25)}$$

Let us now apply these formulas to some typical transmission lines. In the first example we assume phase dispersion is negligible and that the attenuation grows as the square of the frequency and linearly with length, L_A:

$$H_A(\omega) = e^{-\kappa\omega^2 L_A/2}. \quad \text{(A26)}$$

For the baseband case $\alpha_0 = \theta_0 = \alpha_1 = \theta_1 = \theta_2 = \theta_3 = 0$ and $\alpha_2 = -\kappa L_A/2$. From (A25) the RMS duration is doubled when (in agreement with [28]),

$$\frac{\kappa L_A}{2} = 3\frac{\tau^2}{2} \quad \text{or} \quad L_A = \frac{3\tau^2}{\kappa} \quad \text{(baseband)}. \quad \text{(A27)}$$

If our input pulse had a bandwidth of $\mathrm{BW}_{1/e} = 10^{11}$Hz, then from (A14) $\tau = \dfrac{10^{-11}}{\pi}$. If the transmission line had attenuation (which exemplifies the superconducting coaxial line of subsection III-B),

$$\kappa = \frac{2(.111)}{8.686}\left[(2\pi)10^{11}\right]^{-2} = (6.5)10^{-26} \quad (\mathrm{Np} - \mathrm{s}^2)/(\mathrm{km} - \mathrm{rad}^2) \quad \text{(A28)}$$

then $L_A = 465$ km for a baseband pulse. For the same transmission line assume a band-pass pulse with the same bandwidth centered at $\omega_0/2\tau = 10^{11}$ Hz. If we substitute

$$\omega^2 = (\omega - \omega_0)^2 + 2\omega_0(\omega - \omega_0) + \omega_0^2 \quad \text{(A29)}$$

into (A26) we see that $\alpha_0 = \theta_0 = \theta_1 = \theta_2 = \theta_3 = 0$, $\alpha_2 = -\kappa L_A/2$, and $\alpha_1 = -\kappa\omega_0 L_A$. From (A24) we see that the RMS duration is doubled when

$$\frac{\kappa L_A}{2} = 3\frac{\tau}{2} \quad \text{or} \quad L_A = \frac{3\tau^2}{\kappa} \quad \text{(band-pass)}$$

which equals the result (eq. (A27)) for the baseband pulse with this kind of transmission line.

In the next example we consider a rectangular superconducting waveguide as considered in [29, eqs. (36) and (38)]:

$$\alpha = 0.165\left[\frac{f_c}{100\ \mathrm{GH_z}}\right]^3 \frac{\left[1 + (f/f_c)^2\right]}{\sqrt{1 - (f_c/f)^2}} \quad \mathrm{dB/km} \quad \text{(A30)}$$

and

$$\beta = -(2.1)10^6\left[\frac{f_c}{100\ \mathrm{GH_z}}\right]\sqrt{(f/f_c)^2 - 1} \quad \mathrm{rad/km} \quad \text{(A31)}$$

where f_c is the cutoff frequency of the dominant mode in the rectangular waveguide. Following [29], we consider the dispersion at the top end of the recommended waveguide band, $f_1 = 1.86 f_c$, with $f_c = 80$ GHz. Expanding (A30) and (A31) around f_1 we have, for a waveguide of length L_B ($\omega = 2\pi f$),

$$\alpha L_B \approx \alpha_0 + \alpha_1(\omega - \omega_1) + \alpha_2(\omega - \omega_1)^2 \quad \text{(A32)}$$

and

$$\beta L_B \approx \theta_0 + \theta_1(\omega - \omega_1) + \theta_2(\omega - \omega_1)^2 + \theta_3(\omega - \omega_1)^3 \quad \text{(A33)}$$

and using (A24) we find that if $L_B = 1$ km the pulse duration will be doubled for a pulse with bandwidth $\mathrm{BW}_{1/e} = 243$ MHz, which is about half that estimated by eye closure in [29]. The 243 MHz bandwidth limitation is due entirely to θ_2. For example, if phase dispersion is neglected ($\theta_2 = \theta_3 = 0$), the waveguide length could be 715 km and still allow the full 60 GHz usable waveguide bandwidth.

As a final example we consider the use of a periodic waveguide to cause θ_2 to vanish at the operating point. Reference [30] describes a rectangular waveguide periodically loaded with capacitive diaphragms. For a waveguide of width 2.3 mm and height 0.5 mm with 0.36-mm-high diaphragms spaced 1 mm along the guide, the propagation constant for lossless walls is given by

$$\beta l = \arccos\left\{\frac{1.905 - 2\pi f l/c}{0.535}\right\} \quad \text{(A34)}$$

where l = period of waveguide = 1 mm. The phase shift over a length L_c is expanded around frequency f_l ($L_{c_{\mathrm{mm}}}$ is L_c measured in millimeters):

$$\theta = -\beta l\frac{L_c}{l} = \theta_0 + \theta_1 2\pi(f - f_1) + \theta_2[2\pi(f - f_1)]^2 + \theta_3[2\pi(f - f_1)]^3. \quad \text{(A35)}$$

The requirement that $\theta_2 = 0$ at f_1 gives $f_1 = 91$ GHz. Thus in a lossless guide at this operating frequency, (A24) implies a pulse-duration-doubling bandwidth of (for $L_{c_{\text{mm}}} = 10^6$mm)

$$\text{BW}_{1/e} = \frac{1}{\pi\left(\sqrt{3}\,\theta_3\right)^{1/3}} = 773 \text{ MHz.} \qquad \text{(A36)}$$

Thus, although eliminating the quadratic phase term θ_2 with the periodic loading increased the bandwidth to 773 MHz from the 243 MHz of the straight waveguide, it is still small relative to that of the levitated coaxial line. Also, as indicated in [31], which derives the lossless version of (A24), significant pulse distortion occurs when the dispersion is due only to θ_3.

Acknowledgment

The authors would like to thank R. Howard, S. Tewksbury, and L. Hornak for helping them through the theory of superconductivity. Further, they thank R. Linke for providing information on optical fiber properties and I. Kaminow and R. Gitlin for helpful reviews of the manuscript. They are also indebted to P. Henry for lending a good critical ear and to K. Eng for initially suggesting the problem of superconductors in communications.

References

[1] T. Van Duzer, and C. W. Turner, *Principles of Superconductive Devices and Circuits*. North Holland, 1981.
[2] R. D. Parks, Ed., *Superconductivity*. Marcell Dekker, 1969.
[3] J. E. C. Williams, *Superconductivity and Its Applications*. London: Pion, 1970.
[4] L. A. Hornak, S. K. Tewksbury, and M. Hatamian, "Impact of high-T_c superconductors on system communications," *IEEE Trans. Components, Hybrids, Manuf. Technol.*, vol. 11, pp. 412–418, Dec. 1988.
[5] F. London, *Superfluids*. Wiley, 1950.
[6] J. F. Kwak, E. L. Venturini, D. S. Ginley and W. Fu, "Grain decoupling at low magnetic fields in ceramic $YGa_2Cu_3O_{7-\delta}$," in *Novel Superconductivity*, Wolf and Kresin, Eds. Plenum, 1987, pp. 983–991.
[7] C. E. Rice, R. B. van Dover, and G. J. Fisanick, "Superconducting thin films of high T_c cuprates prepared by spin-on/pyrolysis," *Appl. Phys. Lett.*, vol. 51, no. 22, pp. 1842–1844, 1987.
[8] A. I. Braginski, "Study of superconducting oxides at Westinghouse," in *Novel Superconductivity*, Wolf and Kresin, Eds. Plenum, 1987, pp. 935–949.
[9] C. W. Chu *et al.*, "Discovery and physics of superconductivity above 90 K," in *Novel Superconductivity*, Wolf and Kresin, Eds. Plenum, 1987, pp. 581–597.
[10] S. N. Song, *et al.* "High T_c superconductivity in Y-Ba-Cu-O system," *Advanced Ceramic Materials*, vol. 2, no. 3B, pp. 480–491, 1987.
[11] J. D. Kraus and K. R. Carver, *Electromagnetics*. New York: McGraw-Hill, 1973.
[12] N. Marcuvitz, Ed., *Waveguide Handbook*. New York: McGraw-Hill, 1951.
[13] A.V. Bazhenov *et al.*, "Infrared reflectivity, inelastic light scattering and energy gap in a Y-Ba-Cu-O superconductors," in *Novel Superconductivity*, Wolf and Kresin, Eds., Plenum, 1987, pp. 893–896.
[14] R. J. Cava *et al.*, "Bulk conductivity at 91 K in single-phase, oxygen deficient perovskite $Ba_2YCu_3O_{9-\delta}$,"*Phys. Rev. Lett.*, vol. 58, no. 16, pp. 1676–1679, 1987.
[15] *Reference Data for Radio Engineers*, 5th ed., ITT. Howard K. Sams, 1968.
[16] R. J. Allen and N. S. Nahman "Analysis and performance of superconductive coaxial transmission lines," *Proc. IEEE*, Oct. 1964.
[17] D. Halliday and R. Resnick, *Physics Part II*, 3rd ed. Wiley, 1978.
[18] J. Kwo, *et al.*, "Single crystal superconducting $Y_1Ba_2Cu_3O_{7-\delta}$ oxide films by molecular beam epitaxy," in *Novel Superconductivity*, in Wolf and Kresin, Eds. Plenum, 1987, pp. 699–703.
[19] R. C. Weast, *CRC Handbook of Chemistry and Physics*. CRC Press, 1985.
[20] J. M. Wozencraft and I. M. Jacobs, *Principles of Communication Engineering*. Wiley, 1967.
[21] W. B. Davenport and W. L. Root, *An Introduction to the Theory of Random Signals & Noise*. McGraw-Hill, 1958.
[22] T. Li, "Advances in lightwave systems research," *AT&T Tech. J.*, vol. 66, no. 1, pp. 5–18, Jan./Feb. 1987.
[23] T. E. Darcie and M. S. Whalen, "Optimized guided wave communication system," U.S. Patent 4 730 888, 1988.
[24] P. S. Henry, R. A. Linke, and A. H. Gnauck, "Introduction to lightwave systems," in *Optical Fiber Telecommunication II*, S. E. Miller and I. P. Kaminow, Eds. Academic Press, 1988, ch. 21, pp. 781–822.
[25] S. Ramo, J. R. Whinnery, and T. VanDuzer, *Fields and Waves in Communication Electronics*, New York: Wiley, 1965, p. 188.
[26] I. S. Gradshteyn and I. M. Ryzhik, *Table of Integrals, Series, and Products*. New York: Academic Press, 1965, p. 307, f.3.323.2.
[27] A. Papoulis, *The Fourier Integral and Its Applications*. New York: McGraw-Hill, 1962, p. 62.
[28] S. K. Tewksbury, L. A. Hornak, and M. Hatamian, "High T_c superconductors for digital system interconnections," in *Superconductivity: Theory and Applications* Elsevier (in press).
[29] J. H. Winters and C. Rose, "High T_c superconductor waveguides: Theory and applications," submitted to *IEEE Trans. Microwave Theory Tech.*
[30] R. E. Collin, *Field Theory of Guided Waves*. New York: McGraw-Hill, 1960, sec. 9.5.
[31] D. Marcuse, "Pulse distortion in single-mode fibers," *Appl. Opt.*, vol. 19, no. 10, pp. 1653–1660, 1980.

✠

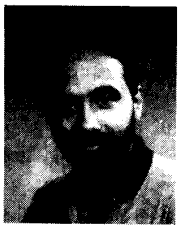

Christopher Rose (S'78–M'86) was born on January 9, 1957, in New York City. He received the B. S. (1979), M. S. (1981), and Ph.D. (1985) degrees from the Massachusetts Institute of Technology, in Cambridge.

He is currently with AT&T Bell Laboratories, Holmdel, NJ, as a member of the Network Systems Research Department. His current technical interests include adaptive connectionist (neural) networks, cellular automata, communications systems and, most recently, applications of high-temperature superconductivity to communications problems.

✠

Michael J. Gans received the B.S. degree in electrical engineering from the University of Notre Dame, IN, in 1957. He then received the M.S. degree in 1961, and the Ph.D. degree in 1965 in electrical engineering from the University of California, Berkeley.

In 1966 he joined Bell Laboratories, Holmdel, NJ, where he has been engaged in research on antennas, mobile radio, and satellite and infrared communications.